Available online at www.sciencedirect.com
ScienceDirect
Dyes and Pigments 74 (2007) 335–342
DYES and PIGMENTS
www.elsevier.com/locate/dyepig

Acrylate photopolymerization on heterostructured TiO_2 photocatalysts

C. Damm [a,*], R. Herrmann [b], G. Israel [c], F.W. Müller [c]

[a] *Friedrich-Alexander-University Erlangen-Nuremberg, Institute of Polymer Materials, Martensstrasse 7, D-91058 Erlangen, Germany*
[b] *Friedrich-Alexander-University Erlangen-Nuremberg, Institute for Chemical Reaction Technique, Egerlandstrasse 3, D-91058 Erlangen, Germany*
[c] *Martin-Luther-University Halle-Wittenberg, Department of Organic Chemistry, Kurt-Mothes-Strasse 2, D-06120 Halle/Saale, Germany*

Received 10 February 2006; received in revised form 14 February 2006; accepted 14 February 2006
Available online 17 April 2006

Abstract

Heterostructured TiO_2 samples were prepared by precipitation of Al_2O_3, Fe_2O_3 hydrate, AgCl and Ag_2O, respectively, onto the surface of a commercial anatase type pigment. The photopolymerization of an ethoxylated trisacrylate was used as a test reaction to check the photocatalytic activity of the heterostructured TiO_2 samples. The TiO_2 sample coated with Al_2O_3 showed no noticeable photocatalytic activity; the untreated TiO_2 was also not a good photocatalyst; in contrast, the TiO_2 samples which had been coated with Fe_2O_3 or AgCl showed enhanced polymerization rate as well as monomer conversion after 120 s illumination. The results of the photopolymerization experiments are explained on the basis of the thermodynamics of the charge transfer between the photoexcited TiO_2 samples and the acrylate. The photoelectric properties of the TiO_2 samples which were characterized using transient Photo-EMF measurements also play an important role in their photocatalytic activity.

Keywords: Photopolymerization; Acrylate; Heterostructured TiO_2; Photo-EMF

1. Introduction

The photopolymerization of pigmented acrylate formulations is of great importance for coating and printing technologies. In most cases such photopaints consist of a mixture of acrylates, the pigment and molecular photoinitiators such as, benzophenone/amines, triarylphosphinoxides and iodonium salts. UV-illumination of these photopaints leads to fragmentation of the initiating compounds which, in turn, results in the formation of reactive species such as radicals or ions which start the polymerization of the acrylates. Although the use of molecular photoinitiators enables photopaint films to be cured very quickly, the use of molecular photoinitiators has attendant disadvantages:

fragments of the photoinitiating compounds remain in the polymer film and can migrate;
the photoinitiators and their fragments can impart odour or color changes to the polymer film; and
most photoinitiators are not suitable for application in the fields of foods and medicine.

Clearly, if the pigment itself was able to start photopolymerization by its photocatalytic activity then no molecular photoinitiators should be necessary. Whilst heterogeneous photocatalyzed polymerizations are known in principle [1–7] they are not widely used. Inorganic [2–7] as well as organic pigments [1] have been employed to initiate the photopolymerization of acrylates [1,3], methacrylates [2,4–7] and other vinylics [3]. Although researchers [2,3,5–7] have shown that heterogeneous photocatalyzed polymerization can be carried out in solution, owing to the use of organic solvents such processes are not suited for practical application.

It has been demonstrated [2,3] that nanoparticles of ZnO, TiO_2 and CdS initiate the photopolymerization of the acrylates

* Corresponding author. Tel.: +49 09131 85 27748; fax: +49 09131 85 28321.
E-mail address: cornelia.damm@ww.uni-erlangen.de (C. Damm).

0143-7208/$ - see front matter © 2006 Elsevier Ltd. All rights reserved.
doi:10.1016/j.dyepig.2006.02.012

and methacrylates better than particles at the micrometer scale. CdS/HgS and CdS/TiO_2 heterostructures were found [5] to be better photoinitiators than pure CdS.

In order to more fully understand both the findings presented by earlier workers [1–7] and the results contained in this paper, an initial discussion of heterogeneous photocatalytic processes seems sensible. In this context, the general scheme of a heterogeneous photocatalytic reaction is displayed in Fig. 1.

Light absorption by the photocatalyst material leads to an excitation of electrons (e^-) from the valence band (VB) into the conduction band (CB). As a consequence, positive holes (h^+) remain in the valence band; electrons and holes can diffuse through the solid followed by trapping or recombination. The generation, diffusion, trapping and recombination of charge carriers due to illumination of the photocatalyst are summarized as photoelectric primary processes. In a second step the charge carriers can be transferred from the catalyst surface to reactants (electron acceptors or donators) such as acrylic monomers.

A photocatalytic reaction is only efficient if electrons and holes are transferred from the catalyst to the reactants by means of suitable electron acceptors and donators, respectively. This charge transfer is possible only if it is thermodynamically possible and if the charge carriers have sufficient lifetime within the surface region. This means that the photoelectric properties of a catalyst material as well as the thermodynamics of charge transfer between the photocatalyst surface and the reactants are important contributors to the efficiency of a heterogeneous photocatalytic reaction. For this reason the results of experiments on photocatalytic reactions must be discussed in terms of both an energy level scheme and the photoelectric properties of the catalyst materials. However, only a few authors have combined investigations of heterogeneous photocatalytic reactions with measurements of the photoelectric properties of the same charges of material used as catalysts [1,8–11].

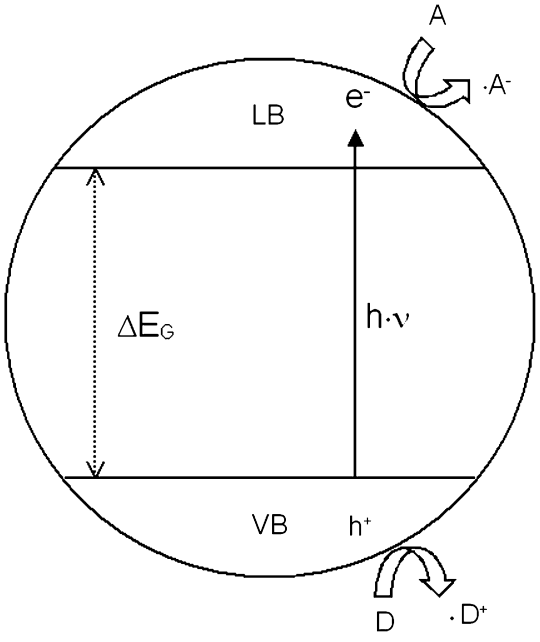

Fig. 1. General scheme of a heterogeneous photocatalytic reaction, VB: valence band, CB: conduction band, ΔE_G: band gap, e^-: electron, h^+: positive hole, A: electron acceptor, D: electron donator, $^{\bullet}A^-$: reduced electron acceptor, $^{\bullet}D^+$: oxidized electron donator.

In this paper we report the heterogeneous photocatalytic polymerization of an ethoxylated trisacrylate using heterostructured TiO_2. Various inorganic compounds were precipitated (about 1% by mass) onto the surface of a commercial anatase type pigment; for comparison, the untreated commercial anatase type pigment was also investigated. The photoelectric primary processes in the TiO_2 samples were characterized using measurements of transient PhotoElectro-Motive Force (Photo-EMF). To perform Photo-EMF measurements the sample is brought into a capacitor and is illuminated by a laser flash through a transparent electrode. The photovoltage is measured as a function of time without any external electric field. As the charge carrier concentration gradient due to the gradient of light absorption and heterojunctions within the sample are the only driving forces for the Photo-EMF generation, this method is well suited to the investigation of influences of the structure of the materials on their photoelectric properties [12].

The amount of the maximum Photo-EMF, U_{max} is a measure of the efficiency of charge separation upon illumination. The Photo-EMF decreases due to recombination or chemical reaction of the charge carriers. The Photo-EMF decay is expressed by a biexponential rate law (Eq. (1)):

$$U(t) = U_1^0 \exp(-k_1 t) + U_2^0 \exp(-k_2 t) \quad (1)$$

By definition, the process with parameters U_1^0 and k_1 is always the faster decay process so that $k_1 > k_2$. In previous works, the faster decay process was assigned to a Photo-EMF in the subsurface region [13,14]; the Photo-EMF method is described in more detail elsewhere [11,13].

2. Experimental

2.1. Materials

The base material was an uncoated anatase type TiO_2 pigment grade K1001 made by Kronos; TiO_2 coated with Al_2O_3 (grade K1014) was also supplied by Kronos. $FeCl_3 \cdot 6H_2O$, $AgNO_3$, NaOH, NaCl, 1,2-dichlorethane and dichloromaleic acid anhydride were purchased from Merck. The pigments and chemicals mentioned above were used as received. The acrylate used (grade SR415) was purchased from Cray Valley; prior to use, inhibitors were removed by filtration over an Al_2O_3 column.

2.2. Coating of TiO_2 with Fe_2O_3 hydrate

101 mg $FeCl_3 \cdot 6H_2O$ was dissolved in 500 ml distilled water; in this solution 2 g of the TiO_2 pigment was dispersed.

The mixture was stirred for 24 h at room temperature and the pigment was then separated by centrifugation (10 min, 5000 rpm) and washed three times with distilled water.

The TiO_2 loaded with Fe^{3+} ions was dispersed in 200 ml of 0.1 N NaOH. After immersion into the NaOH the pigment becomes immediately brownish showing the presence of Fe_2O_3 hydrate. After 1 h of stirring at room temperature, the pigment was separated by centrifugation (10 min, 5000 rpm), washed with distilled water and dried in a desiccator. The coated TiO_2 (1 g) was heated to 220 °C/24 h to transform the Fe_2O_3 hydrate into Fe_2O_3.

2.3. Coating of TiO_2 with AgCl and Ag_2O, respectively

The coating of TiO_2 with AgCl as well as Ag_2O was carried out in the absence of daylight. For coating with AgCl, 12 mg of $AgNO_3$ and for coating with Ag_2O 15 mg of $AgNO_3$ were dissolved in 100 ml distilled water. In each case, 1 g of the TiO_2 pigment was dispersed in the ensuing solution. The mixture was stirred for 24 h at room temperature and the pigment was then separated by centrifugation (10 min, 5000 rpm) and washed with distilled water. The Ag^+ ion loaded TiO_2 samples were immersed in 100 ml of 0.1 N NaCl and 0.1 N NaOH, respectively, and stirred for 1 h at room temperature, after which, they were separated by centrifugation (10 min, 5000 rpm), washed with distilled water and dried at 110 °C for 3 h.

2.4. Determination of the amounts of coating materials deposited on the TiO_2 surface

To determine the amounts of Fe^{3+} as well as Ag^+ ions deposited on the TiO_2 surface, the Fe^{3+} as well as the Ag^+ content of the solution was measured after the adsorption experiment. The Fe^{3+} content was determined photometrical using a Shimadzu UV-3101 PC, employing complex forming reaction with SCN^-. The Ag^+ content was determined by means of anodic stripping voltammetry using a glassy carbon electrode as working electrode, Ag/AgCl as reference electrode and Pt-wire as counter electrode.

2.5. Structural analyses

Powder X-ray diffraction (XRD) was used to detect the crystal type of the TiO_2 samples. The X-ray diffraction patterns were recorded on a Phillips X'Pert Pro MPD X-ray diffractor in the range of 2Θ between 10° and 70° using Cu $K\alpha_1$ irradiation. A combination of scanning electron microscopy (SEM) and EDX (Oxford Instruments) was used to investigate the morphology of the TiO_2 and to detect the coating materials.

2.6. Photo-EMF measurements

Photo-EMF measurements were undertaken using pigment polymer dispersion layers, employing polyvinyl butyral as polymeric binder. The layers were prepared by a solution casting process using 1,2-dichlorethane as solvent. The dispersion layers used contained about 25% pigment by mass, were 60–80 μm thick and displayed total absorption in the UV range.

From the layer, pieces measuring 10 mm in diameter were cut and brought into the Photo-EMF device. The sample was illuminated by a single flash of a nitrogen laser PNL 100 made by Lasertechnik Berlin GmbH (wavelength: 337 nm, pulse duration: 300 ps, power: 100 kW). The light intensity at the sample's place was about 3×10^{13} quanta per flash; the temperature of the sample and the amplifier was 25 °C.

All Photo-EMF signals and parameters presented herein were the mean values of three measurements; for each measurement a new piece of the layer was used. The Photo-EMF device is constructed like a capacitor with one transparent electrode. The Photo-EMF is measured without any external electric field (i.e. contactless) by insulating foils between the sample and the electrodes; see Ref. [13] for further details of the Photo-EMF device and the measurement procedure used.

2.7. Photopolymerization

Polymerization of the trisacrylate **1** was used to investigate the photocatalytic activity of the TiO_2 samples. As a promoting agent 6.5 mol% of the electron acceptor dichloromaleic acid anhydride **2** was added to the acrylate (see Section 3.4).

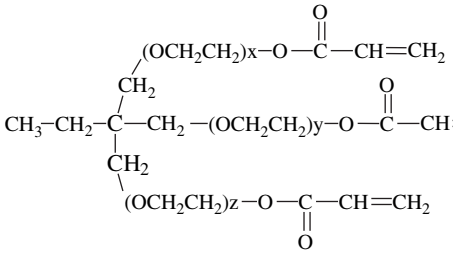

1

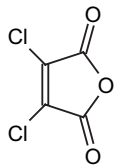

2

The sample contained 5.5% by mass of the TiO_2 investigated; as a comparison, polymerization of the mixture was attempted without TiO_2. For the polymerization experiments, films of the pigment monomer mixture of layer thickness 20 μm were prepared using a knifecoater. The layers were illuminated by white light from a Mercury high pressure lamp (power 100 W); to avoid direct excitation of the acrylate,

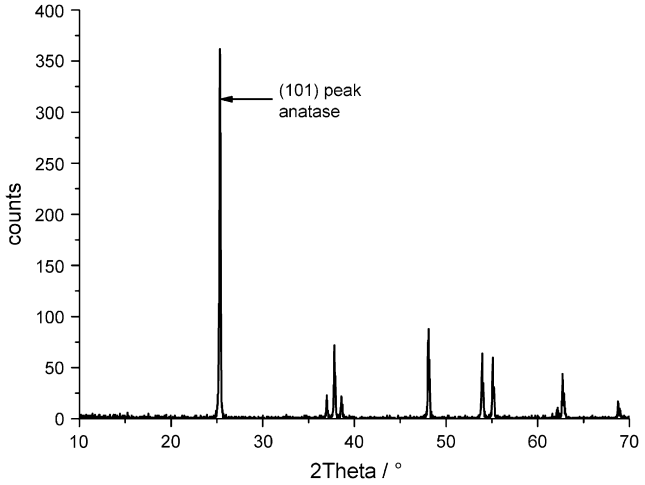

Fig. 2. X-ray diffraction pattern of a powder sample of untreated TiO_2.

radiation with wavelengths shorter than 350 nm was removed using a cut-off filter. The light intensity at the sample was 90 mW cm^{-2}.

The relative concentration of double bonds was measured by real time infrared spectroscopy using a Biorad FTS6000 spectrometer; the intensity of the absorption band at 810 cm^{-1} (C–H wagging vibration of an unsaturated carbon atom) was monitored as a function of illumination time. To exclude oxygen from air the sample chamber was purged with nitrogen 3 min before the measurement begun as well as during the measurement procedure. All results of the polymerization experiments presented here are the mean values of three attempts.

3. Results and discussion

3.1. Amount of the coating materials deposited on the TiO_2 surface

The analyses described in Section 2.4 provided the following results. After the adsorption process no Fe^{3+} ions were detected in solution from which it can be concluded that the full amount of Fe^{3+} ions had been adsorbed onto the TiO_2 surface, which corresponds to 1% by mass of Fe_2O_3.

In the wash water no Ag^+ ions were detected and the supernatant contained 4.4% of the original Ag^+ used in the AgCl coating and 23.8% of the original Ag^+ used in the Ag_2O coating. These values correspond to an AgCl quantity of 0.97% by mass and an Ag_2O quantity of 0.78% by mass on the TiO_2, respectively. The Al_2O_3 content of the commercial Al_2O_3 coated TiO_2 amounts to 1.4% by mass according to the supplier.

3.2. Structure of the TiO_2 samples

The X-ray diffraction pattern of the neat TiO_2 showed a diffraction peak at $2\Theta = 25.33°$ which is the (101) diffraction of the anatase type (Fig. 2); because at $2\Theta = 27.42°$ there was no diffraction peak, there was no rutile form of the pigment present in the sample.

The X-ray diffraction patterns of the coated samples agree completely with that of the untreated sample which shows that the coatings cannot be detected using XRD. One reason for this is the amorphous nature of the coatings in the cases of the Al_2O_3 and Fe_2O_3 hydrates. Although the Fe_2O_3, AgCl and Ag_2O should be crystalline, the amounts of the coating materials in the samples were below the detection level of XRD.

Fig. 3a shows an SEM micrograph of the untreated TiO_2 which reveals the spherical primary particles having sizes of about 200 nm formed large agglomerates. The presence of the coating materials did not change the morphology of the TiO_2, as exemplified by the SEM micrograph of the TiO_2 sample coated with Fe_2O_3 shown in Fig. 3b.

The presence of the coating materials Al, Fe or Ag on the TiO_2 samples was proven qualitatively by means of EDX. The EDX analysis of the neat TiO_2 revealed that this sample consists only of Ti and O; impurities could not be detected.

3.3. Photoelectric properties

Fig. 4a shows the Photo-EMF signals of the TiO_2 samples recorded in the time range of up to 100 ms after the laser flash.

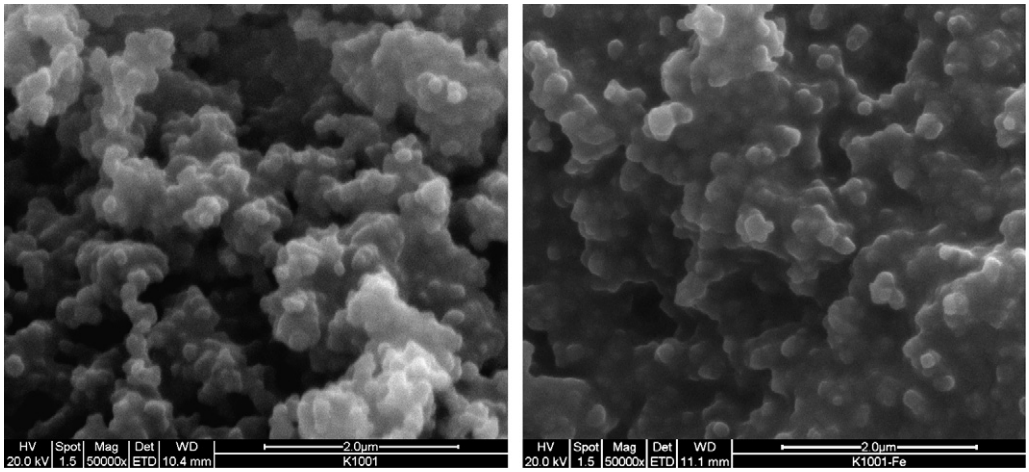

Fig. 3. SEM micrograph of a powder sample of (a) untreated TiO_2 and (b) TiO_2 coated with 1% by mass Fe_2O_3.

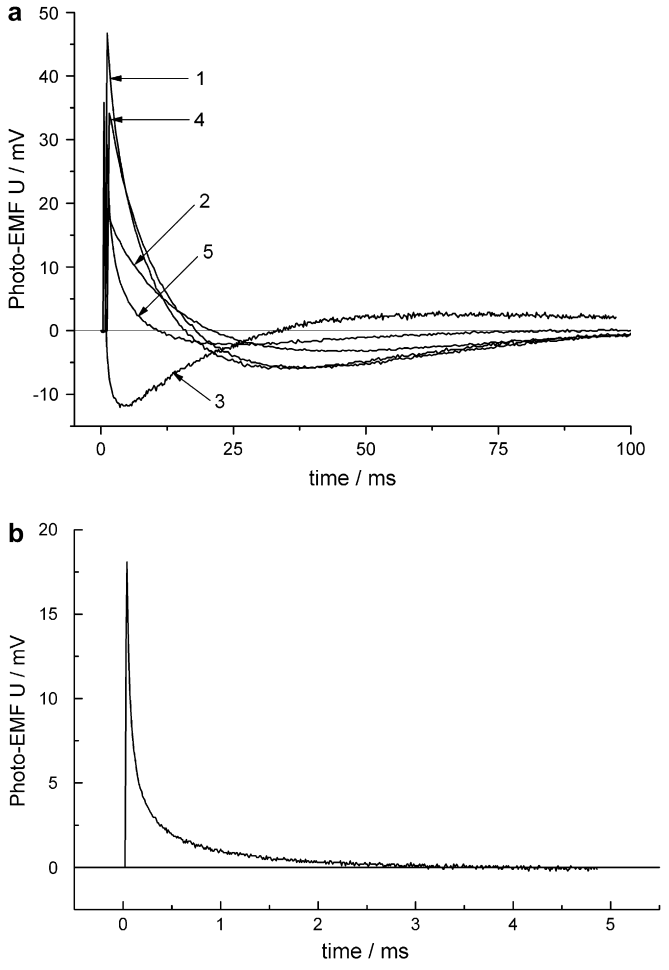

Fig. 4. (a) Photo-EMF signals of coated TiO_2 samples in comparison to untreated TiO_2, excitation wavelength: 337 nm, laser flash intensity at the samples place: 3×10^{13} quanta per flash, curve 1: neat TiO_2, curve 2: 1.4% by mass Al_2O_3 on TiO_2, curve 3: 1.0% by mass Fe_2O_3 on TiO_2, curve 4: 0.97% by mass AgCl on TiO_2, curve 5: 0.78% by mass Ag_2O on TiO_2. (b) Photo-EMF signal of a TiO_2 sample coated with 1.0% by mass Fe_2O_3 hydrate.

As the time range shown in Fig. 4a is not suited to visualize the Photo-EMF decay of the TiO_2 sample coated with 1.0% by mass Fe_2O_3 hydrate, the signal is shown in a separate figure (Fig. 4b). The parameters of the signals shown in Fig. 4a and b are summarized in Table 1.

The results shown in Fig. 4a, b and Table 1 can be summarized as follows. All of the TiO_2 samples show Photo-EMF signals starting with a positive sign which means that all of the samples behaved as n-type photoconductors which is typical for TiO_2. Whilst the coating materials used in this work were not able to change the type of photoconduction in TiO_2, the coating materials, nevertheless, changed the photoelectric properties of the TiO_2 although the amounts of those materials are low. Generally, the maximum values U_{max} for the Photo-EMF of the coated samples were lower than that of the untreated sample. Deposition of Al_2O_3 caused the strongest decrease of U_{max}; this decrease could signify a reduction in the efficiency of charge separation due to the coating. Another reason for a decrease in U_{max} could be charge transfer between the TiO_2 and the coating material.

Although from the values of U_{max}, it can only be concluded that the coatings should change the photocatalytic activity of TiO_2, it is difficult to predict if the photocatalytic activity was increased or decreased by coating. The coating of TiO_2 strongly influenced the Photo-EMF decay kinetics: deposition of Fe_2O_3 hydrate increased k_1 by two orders of magnitude whereas in contrast, coating with Al_2O_3, AgCl or Ag_2O led to a decrease in k_1. The finding that in general, the coating of TiO_2 altered the value of k_1 more than the value of k_2, confirms our previous result that k_1 may be assigned to a Photo-EMF in the subsurface region.

The TiO_2 sample coated with 1.0% by mass Fe_2O_3 showed a complex Photo-EMF signal comprising two crossing points with zero potential; such behaviour may be a hint at a heterojunction in the sample.

3.4. Photopolymerization

Fig. 5 shows the relative concentration of double bonds as a function of illumination time for samples consisting of the acrylate **1**, the electron acceptor **2** and the TiO_2 samples mentioned; the kinetics of the photopolymerization of a blank sample is shown too.

If the pigment is photocatalytic active the pigmented sample must polymerize faster than the reference without pigment.

The maximum polymerization rate r_P^{max} was determined by differentiating the curves shown in Fig. 5. Moreover, the double bond conversion after an illumination time of 120 s $C_{120\ s}$ was determined from the experimental curves. The results are summarized in Table 2.

The sample pigmented with neat TiO_2 polymerized faster than the pigment free reference but the difference was not very large. This shows that the neat TiO_2 has only small photocatalytic activity; this behaviour was expected because this pigment is not optimised for application in heterogeneous photocatalysis.

Coating TiO_2 with Al_2O_3 lowered the photopolymerization rate in comparison to neat TiO_2, corresponding to the results discussed previously [15]. Coating with Al_2O_3 suppressed the photocatalytic activity of TiO_2 and, therefore, TiO_2 coated with Al_2O_3 can be used for applications where the photocatalytic activity of TiO_2 would be detrimental.

In the case of the sample containing TiO_2 coated with Fe_2O_3 hydrate the monomer conversion was rather low in comparison to the reference. This sample showed nearly no photocatalytic activity but acted as a light filter which suppressed homogeneous polymerization. This poor photocatalytic behaviour can be explained by the extreme short charge carrier lifetimes in this sample, as described in Section 3.3. So the charge carriers recombine before they can be transferred to the monomer.

If the Fe_2O_3 hydrate on top of the TiO_2 is converted into Fe_2O_3 by a heating process, a remarkable increase in polymerization rate r_P^{max} and monomer conversion $C_{120\ s}$ is observed, showing that a photocatalytic inactive material can be changed into an active one in a simple way. The TiO_2 coated with AgCl shows the best photocatalytic activity: In comparison to all

Table 1
Maximum values U_{max} and kinetic parameters of the Photo-EMF curves shown in Fig. 4a and b

Curve no. in Fig. 4a	Sample	U_{max} (mV)	U_1^0 (mV)	U_2^0 (mV)	k_1 (s^{-1})	k_2 (s^{-1})
1	Neat TiO_2	46.7 ± 3.3	63 ± 7	-16 ± 2	117 ± 1.2	26.2 ± 0.3
2	$TiO_2 + 1.4$ wt% Al_2O_3	19.2 ± 1.4	255 ± 28	-253 ± 32	44.9 ± 0.5	44.5 ± 0.5
Curve in Fig. 4b	$TiO_2 + 1$ wt% Fe_2O_3 hydrate	28.5 ± 2.0	24 ± 3	4 ± 0.5	$(2.1 \pm 0.1) \times 10^4$	$(1.6 \pm 0.1) \times 10^3$
3	$TiO_2 + 1$ wt% Fe_2O_3[a]	36.0 ± 2.5	38 ± 4	-2 ± 0.2	$(2.7 \pm 0.1) \times 10^3$	65.7 ± 0.7
4	$TiO_2 + 0.97$ wt% AgCl	34.1 ± 1.9	5052 ± 1662	-5018 ± 1661	53.5 ± 0.3	53.2 ± 0.4
5	$TiO_2 + 0.78$ wt% Ag_2O	30.3 ± 1.8	47 ± 5	-16 ± 4	96.3 ± 6.6	31.6 ± 1.6

[a] Photo-EMF signal contains two crossing points with zero potential. For that reason it cannot be described completely by Eq. (1). The parameters mentioned in Table 1 describe the signal from its maximum value up to the second crossing point with zero potential.

other samples investigated in this work, both the polymerization rate and the monomer conversion were highest.

Thus, the results presented in this work show that the photocatalytic activity of TiO_2 can be enhanced or suppressed by coating with suitable materials. To understand the results of the photopolymerization experiments the thermodynamics of charge transfer between the photoexcited TiO_2 and the acrylate must be taken into account. In Fig. 6 the energy levels of the valence and conduction band edges as well as the band gap energies ΔE_G are shown for TiO_2 and the coating materials used in this work [16–21]. Moreover, Fig. 6 shows the energetic positions of the highest occupied molecular orbital (HOMO) and the lowest unoccupied molecular orbital (LUMO) of the acrylate.

The shortest light wavelength used was 350 nm, meaning that the highest available photon energy was 3.5 eV. Whilst this energy was not sufficient to transfer electrons from the HOMO to the LUMO of the acrylate, it was sufficiently high for interband excitation to occur in the TiO_2. The upper edge of the valence band of TiO_2 lies below the HOMO of the acrylate; this means that holes from the valence band of the photoexcited TiO_2 can be transferred to the HOMO of the acrylate. This process leads to oxidation of the acrylate and, in this way, radical cations are formed which can initiate polymerization. However, TiO_2 is not able to transfer electrons from its conduction band into the LUMO of the acrylate because the LUMO of the acrylate is located at a higher energy level than the conduction band of the TiO_2. Consequently, an electron acceptor such as dichloromaleic acid anhydride must be added to trap the electrons in the TiO_2. Indeed, without the electron acceptor no remarkable photopolymerization of the acrylate is observed in the presence of TiO_2 because the photocatalytic process is stopped by the negative charging of the TiO_2.

The light used is not able to excite electrons from the valence band into the conduction band of Al_2O_3. Moreover, an electron or hole transfer between Al_2O_3 and the photoexcited TiO_2 is forbidden thermodynamically, because the valence band of Al_2O_3 lies below that of the TiO_2 and the conduction band of Al_2O_3 lies above that of TiO_2. Hence, the Al_2O_3 does not contain any free charge carrier which could be transferred to the acrylate. However, the efficiency of direct charge transfer between the TiO_2 and the acrylate is reduced because the Al_2O_3 partially covers the active TiO_2 surface and so no charge transfer can occur at the covered places between the TiO_2 and the reactants.

In the case of TiO_2 coated with Fe_2O_3, AgCl or Ag_2O, the incident light causes interband excitation of electrons in the TiO_2 as well as in the coating. Here the different positions of the energy bands of the coatings govern the photocatalytic activity of the coated samples. Coating with Fe_2O_3 increases the photocatalytic activity of TiO_2 although the upper edge of valence band of Fe_2O_3 is located above the HOMO of the acrylate. However, in this case, it must be considered that in Fe_2O_3 the incident light is able to promote electrons into the conduction band which are located 1.2 eV below the upper edge of the valence band, which means that electrons have an energy level of about −8.2 eV. Consequently in the photoexcited Fe_2O_3 coating, holes in the valence band having energy levels above −8.2 eV are available which can be transferred to the acrylate to form initiating radical cations. Thus, the TiO_2 as well as the coating material are able to oxidize the acrylate, resulting in enhanced photocatalytic activity.

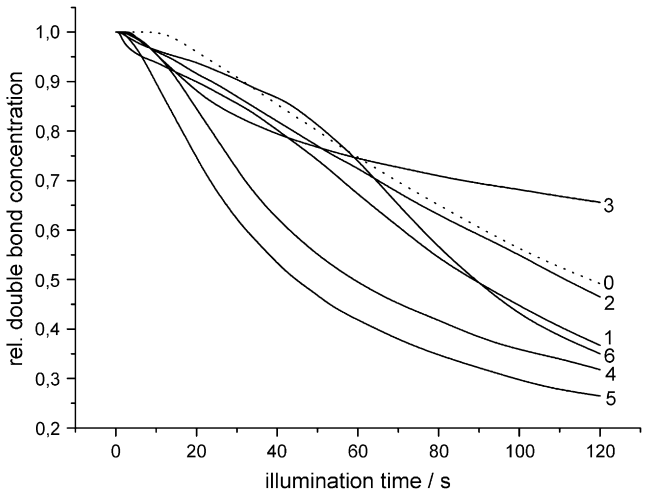

Fig. 5. Kinetics of the photopolymerization of the acrylate **1** pigmented with 5.5% by mass of the TiO_2 samples mentioned (solid lines): curve 1: neat TiO_2, curve 2: 1.4% by mass Al_2O_3 on TiO_2, curve 3: 1.0% by mass Fe_2O_3 hydrate on TiO_2, curve 4: 1.0% by mass Fe_2O_3 on TiO_2, curve 5: 0.97% by mass AgCl on TiO_2, curve 6: 0.78% by mass Ag_2O on TiO_2. The dotted line shows the polymerization kinetics of the acrylate without TiO_2 but in the presence of the electron acceptor **2** (curve 0).

Table 2
Maximum rate of the photopolymerization r_p^{max} and double bond conversion after 120 s illumination $C_{120\,s}$ of the acrylate samples mentioned in Fig. 5

Curve no. in Fig. 5	Sample	$r_{max}^{P}/[M]_0$ (s^{-1})	$C_{120\,s}$ (%)
0	Without TiO_2	$(5.5 \pm 0.3) \times 10^{-3}$	50.8 ± 2.5
1	Neat TiO_2	$(6.8 \pm 0.3) \times 10^{-3}$	63.3 ± 3.2
2	$TiO_2 + 1.4$ wt% Al_2O_3	$(5.0 \pm 0.3) \times 10^{-3}$	53.5 ± 2.7
3	$TiO_2 + 1$ wt% Fe_2O_3 hydrate	$(8.0 \pm 0.4) \times 10^{-3}$	34.4 ± 1.7
4	$TiO_2 + 1$ wt% Fe_2O_3	$(1.2 \pm 0.1) \times 10^{-2}$	68.2 ± 3.4
5	$TiO_2 + 0.97$ wt% AgCl	$(1.4 \pm 0.1) \times 10^{-2}$	73.5 ± 3.7
6	$TiO_2 + 0.78$ wt% Ag_2O	$(7.7 \pm 0.4) \times 10^{-3}$	65.0 ± 3.3

In contrast, the coatings of AgCl and Ag_2O cannot transfer electrons or holes to the acrylate in the photoexcited state and so, in these cases, a reduction in the photocatalytic activity of the sample would be expected (like in the case of Al_2O_3 coated TiO_2); for the sample coated with Ag_2O this was observed. However, in the case of the TiO_2 coated with AgCl, enhanced photocatalytic activity was recorded. This can be explained in terms of charge transfer between the TiO_2 and the AgCl. The photoexcited TiO_2 is able to transfer holes to the AgCl. From a chemical point of view this hole transfer corresponds to the oxidation of chloride ions to chlorine atoms; as chlorine atoms are reactive radical species they should be able to initiate the acrylate polymerization.

The results show that for an explanation of the photocatalytic activity of a coated sample the thermodynamics of the charge transfer between the basis material, the coating material and the reactants must be discussed. Moreover, charge transfer between the basis photocatalyst and the coating material must also be taken into account.

4. Conclusions

Coating TiO_2 with a small amount of inorganic compounds can enhance or reduce its ability to initiate acrylate polymerization. Thus, the coating of photocatalytic active pigments can be a way to achieve photopolymerization processes without recourse to a molecular photoinitiator. However, the polymerization rates achieved using coated TiO_2 pigments are low in comparison to samples containing photoinitiators. To substitute photoinitiators with photocatalytic active pigments, more research is needed to improve the photocatalytic activity of the pigments. One way to achieve this could be to optimise the amount of Fe_2O_3 or AgCl coating used as the affect of the coating material on the photocatalytic activity of the TiO_2 corresponding to that of its photoelectric properties, as proven by Photo-EMF measurements. This can be explained on the basis of the thermodynamics of charge transfer between the photoexcited catalyst samples and the acrylate.

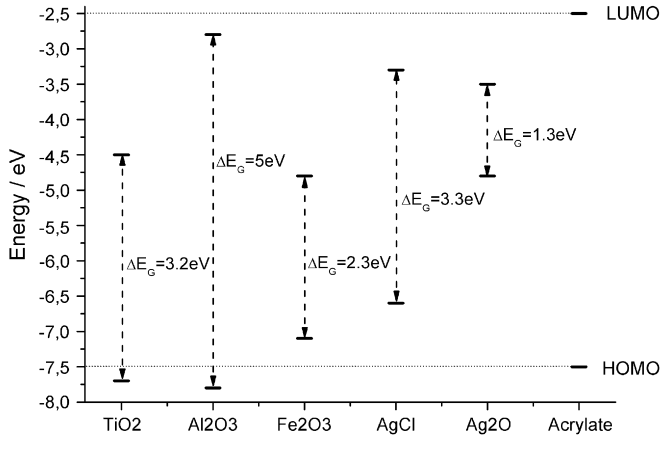

Fig. 6. Energy levels of the upper edge of the valence band (lower bar), the lower edge of the conduction band (upper bar) and band gap energies ΔE_G for TiO_2 and the coating materials used in this work [16–21]. The locations of the highest occupied molecular orbital (HOMO) and lowest unoccupied molecular orbital (LUMO) of the acrylate are shown on the right side of the scheme.

Acknowledgements

The authors are grateful to the German Research Foundation (DFG) and the county Sachsen-Anhalt for financial support of this work. The authors also acknowledge Prof. Dr. R. Mehnert and Dr. T. Scherzer from the Institute of Surface Modification (IOM Leipzig) for the opportunity to perform photopolymerization experiments using time-resolved IR-spectroscopy. Thanks are also due to Mrs. E. Springer from the Institute of Glass and Ceramics of the University Erlangen for providing the SEM micrographs and carrying out the EDX investigations.

References

[1] Rosche K, Decker C, Israel G, Fouassier J-P. Pigment polymer layers as sensitizers for the photopolymerization of trimethylolpropane triacrylate. Eur Polym J 1997;33(6):849–56.
[2] Hoffman AJ, Yee H, Mills G, Hoffmann MR. Photoinitiated polymerisation of methyl methacrylate using Q-sized ZnO colloids. J Phys Chem 1992;96:5540–6.
[3] Hoffman AJ, Yee H, Mills G, Hoffmann MR. Q-sized CdS. Synthesis, characterization and efficiency of photoinitiation of polymerisation of several vinylic monomers. J Phys Chem 1992;96:5546–52.
[4] Bellobono IR, Morelli R, Chiodaroli CM. Photocatalysis and promoted photocatalysis during photocrosslinking of multifunctional acrylates in composite membranes immobilising titanium dioxide. J Photochem Photobiol A 1997;105:89–94.
[5] Popovic IG, Katsikas L, Weller H. The photopolymerisation of methacrylic acid by colloidal semiconductors. Polym Bull 1994;32:597–603.
[6] Huang ZY, Barber T, Mills G, Morris M-B. Heterogeneous photopolymerisation of methyl methacrylate initiated by small ZnO particles. J Phys Chem 1994;98:12746–52.
[7] Qu JF, Zhang SW, Song JH, Huang W. Solar photocatalytic polymerization of methyl methacrylate in aqueous medium with TiO_2/Na_2SO_3 system. Acta Polym Sin 2001;5:656–9.
[8] Laubrich J, Israel G. Heterogeneous photocatalysis – a multifactorial problem. J Inf Rec 1998;24:427–34.
[9] Wilke K, Breuer HD. The photocatalytic behaviour of titania–silica mixed oxides. J Inf Rec 1998;24:309–14.
[10] Wilke K, Breuer HD. The influence of transition metal doping on the physical and photocatalytic properties of titania. J Photochem Photobiol A 1999;121:49–53.
[11] Schiller M, Mueller FW, Damm C. Photo-physics of surface-treated titanium dioxides. J Photochem Photobiol A 2002;149:227–36.

[12] Damm C, Mueller FW, Israel G, Abicht HP. Structural influences on the photoelectric properties of TiO_2. Dyes Pigments 2003;56:151–7.
[13] Israel G, Mueller FW, Damm C, Harenburg J. Measurement problems and kinetic treatment of Photo-E.M.F. curves. J Inf Rec 1997;23: 559–84.
[14] Mueller FW, Damm C, Israel G. The role of traps in the interpretation of Photo-E.M.F. parameters of organic dye pigments. J Inf Rec 2000;25: 533–52.
[15] Gesenhues U. Al-doped TiO_2 pigments: influence of doping on the photocatalytic degradation of alkyd resins. J Photochem Photobiol A 2001;139:243–51.
[16] Hagfeldt A, Grätzel M. Light-induced redox reactions in nanocrystalline systems. Chem Rev 1995;95:49–68.
[17] Fox MA. Top Curr Chem 1987;142:71.
[18] Dobos D. Electrochemical data, a handbook for electrochemists in industry and universities. Budapest: Akademiai Kiado; 1975.
[19] Lanz M, Schürch O, Calzaferri G. Photocatalytic oxidation of water to O_2 on AgCl-coated electrodes. Photochem Photobiol A 1999;120:105–17.
[20] Tjeng LH, Meinders MBJ, van Elp J, Ghijsen J, Sawatzky GA. Electronic structure of Ag_2O. Phys Rev B 1990;41(5):3190–9.
[21] The elements and native oxides. In: Handbooks of monochromatic XPS spectra series, vol. 1. California: XPS International Inc.; 1999.